


# Subclinical effects of long-chain fatty acid $\beta$ -oxidation deficiency on the adult heart: A case-control magnetic resonance study

Suzan J. G. Knottnerus<sup>1,2</sup> | Jeannette C. Bleeker<sup>1,2</sup> | Sacha Ferdinandusse<sup>2</sup> | Riekelt H. Houtkooper<sup>2</sup> | Mirjam Langeveld<sup>3</sup> | Aart J. Nederveen<sup>4</sup> | Gustav J. Strijkers<sup>5</sup> | Gepke Visser<sup>1,2</sup> | Ronald J. A. Wanders<sup>2</sup> | Frits A. Wijburg<sup>6</sup> | S. Matthijs Boekholdt<sup>7</sup> | Adrianus J. Bakermans<sup>4</sup> 

<sup>1</sup>Department of Metabolic Diseases, Wilhelmina Children's Hospital, University Medical Center Utrecht, Utrecht, The Netherlands

<sup>2</sup>Laboratory Genetic Metabolic Diseases, Amsterdam University Medical Centers, University of Amsterdam, Amsterdam Gastroenterology and Metabolism, Amsterdam, The Netherlands

<sup>3</sup>Department of Endocrinology and Metabolism, Amsterdam University Medical Centers, University of Amsterdam, Amsterdam, The Netherlands

<sup>4</sup>Department of Radiology and Nuclear Medicine, Amsterdam University Medical Centers, University of Amsterdam, Amsterdam, The Netherlands

<sup>5</sup>Biomedical Engineering and Physics, Amsterdam University Medical Centers, University of Amsterdam, Amsterdam, The Netherlands

<sup>6</sup>Department of Pediatrics, Emma Children's Hospital, Amsterdam University Medical Centers, University of Amsterdam, Amsterdam, The Netherlands

<sup>7</sup>Department of Cardiology, Amsterdam University Medical Centers, University of Amsterdam, Amsterdam, The Netherlands

## Correspondence

Adrianus J. Bakermans, Department of Radiology and Nuclear Medicine (Z0-180), Amsterdam University Medical Centers, University of Amsterdam, Meibergdreef 9, 1105 AZ Amsterdam, The Netherlands.  
Email: a.j.bakermans@amsterdamumc.nl

**Communicating Editor:** Manuel Schiff

## Funding information

Netherlands Organisation for Scientific Research (NWO), Grant/Award Number: 91617155

## Abstract

Cardiomyopathy can be a severe complication in patients with long-chain fatty acid  $\beta$ -oxidation disorders (LCFAOD), particularly during episodes of metabolic derangement. It is unknown whether latent cardiac abnormalities exist in adult patients. To investigate cardiac involvement in LCFAOD, we used proton magnetic resonance imaging (MRI) and spectroscopy (<sup>1</sup>H-MRS) to quantify heart function, myocardial tissue characteristics, and myocardial lipid content in 14 adult patients (two with long-chain 3-hydroxyacyl-CoA dehydrogenase deficiency (LCHADD); four with carnitine palmitoyltransferase II deficiency (CPT2D); and eight with very long-chain acyl-CoA dehydrogenase deficiency (VLCADD)) and 14 gender-, age-, and BMI-matched control subjects. Examinations included cine MRI, MR tagging, native myocardial T<sub>1</sub> and T<sub>2</sub> mapping,

**Abbreviations:** <sup>1</sup>H-MRS, proton magnetic resonance spectroscopy; ATP, adenosine triphosphate; BSA, body surface area; CPT2D, carnitine palmitoyltransferase II deficiency; DCM, dilated cardiomyopathy; ECG, electrocardiography; EDV, end-diastolic volume; EF, ejection fraction; ESV, end-systolic volume; GLS, global longitudinal strain; HCM, hypertrophic cardiomyopathy; LCFAOD, long-chain fatty acid  $\beta$ -oxidation disorder; LCHADD, long-chain 3-hydroxyacyl-CoA dehydrogenase deficiency; LCT, long-chain triglyceride; LV, left ventricular/left ventricle; MCT, medium-chain triglyceride; MOLLI, modified Look-Locker inversion recovery; MRI, magnetic resonance imaging; PRESS, point-resolved spectroscopy; RV, right ventricular/right ventricle; SV, stroke volume; TE, echo time; TR, repetition time; TSR, torsion-to-shortening ratio; VLCADD, very long-chain acyl-CoA dehydrogenase deficiency.

This is an open access article under the terms of the Creative Commons Attribution-NonCommercial License, which permits use, distribution and reproduction in any medium, provided the original work is properly cited and is not used for commercial purposes.

© 2020 The Authors. *Journal of Inherited Metabolic Disease* published by John Wiley & Sons Ltd on behalf of SSIEM

and localized  $^1\text{H-MRS}$  at 3 Tesla. Left ventricular (LV) myocardial mass ( $P = .011$ ) and the LV myocardial mass-to-volume ratio ( $P = .008$ ) were higher in patients, while ejection fraction (EF) was normal ( $P = .397$ ). LV torsion was higher in patients ( $P = .026$ ), whereas circumferential shortening was similar compared with controls ( $P = .875$ ). LV hypertrophy was accompanied by high myocardial  $T_1$  values (indicative of diffuse fibrosis) in two patients, and additionally a low EF in one case. Myocardial lipid content was similar in patients and controls. We identified subclinical morphological and functional differences between the hearts of LCFAOD patients and matched control subjects using state-of-the-art MR methods. Our results suggest a chronic cardiac disease phenotype and hypertrophic LV remodeling of the heart in LCFAOD, potentially triggered by a mild, but chronic, energy deficiency, rather than by lipotoxic effects of accumulating lipid metabolites.

#### KEYWORDS

energy deficiency, fibrosis, left ventricular hypertrophy, lipids, magnetic resonance imaging, mitochondrial fatty acid  $\beta$ -oxidation, torsion

## 1 | BACKGROUND

Long-chain fatty acid  $\beta$ -oxidation disorders (LCFAODs) are inborn errors of metabolism causing defects in one of the enzymes involved in transport or oxidation of long-chain fatty acids. These enzymes are essential for mitochondrial adenosine triphosphate (ATP) production from fatty acids, and LCFAODs are commonly characterized by an impaired energy homeostasis and accumulation of lipid metabolites.<sup>1,2</sup> The most common LCFAODs are carnitine palmitoyltransferase II deficiency (CPT2D; OMIM 600650), very long-chain acyl-CoA dehydrogenase deficiency (VLCADD; OMIM 609575), and long-chain 3-hydroxyacyl-CoA dehydrogenase deficiency (LCHADD; OMIM 609016). Many newborn screening programs worldwide currently include these LCFAODs.<sup>3</sup> Clinical symptoms typically arise or are exacerbated in catabolic conditions and include hypoketotic hypoglycemia, rhabdomyolysis, and hypertrophic cardiomyopathy (HCM) as well as dilated cardiomyopathy (DCM).<sup>4</sup> To date, little is known about the pathophysiology of cardiac complications in LCFAODs.

Similar to lipotoxicity in diabetic cardiomyopathy,<sup>5</sup> an excessive accumulation of lipid metabolites may have detrimental effects on the myocardium in LCFAODs. So far, myocardial lipid accumulation in LCFAOD patients has only been observed in autopsy of CPT2D and VLCADD patients.<sup>6-8</sup> Furthermore, histological analyses of LCFAOD mouse models revealed myocardial microvesicular lipid accumulation,<sup>9-11</sup> left ventricular (LV) hypertrophy, and myocardial fibrosis.<sup>9</sup> Taken together, those results point to a role for lipotoxicity as a pathologic mediator of

#### Synopsis

A comprehensive noninvasive cardiac magnetic resonance imaging protocol identified subclinical morphological and functional differences between the hearts of patients with long-chain fatty acid  $\beta$ -oxidation disorders and their gender-, age-, and BMI-matched controls.

cardiomyopathy in LCFAOD. This was corroborated by proton magnetic resonance imaging (MRI) and spectroscopy ( $^1\text{H-MRS}$ ) measurements of in vivo myocardial lipid accumulation in a long-chain acyl-CoA dehydrogenase knock-out mouse model with LV hypertrophy and impaired cardiac performance.<sup>12,13</sup> In light of those studies, it is conceivable that accumulation of lipid metabolites in inborn errors of fatty acid  $\beta$ -oxidation may contribute to the development of cardiac complications.

The heart derives the majority of its energy from mitochondrial fatty acid  $\beta$ -oxidation, which implies that insufficient ATP synthesis by an impaired fatty acid  $\beta$ -oxidation capacity may disturb the myocardial energy homeostasis, particularly during catabolic stress. Even in the absence of catabolic stress, myocardial energy deficiency has been reported for LCFAOD mouse models,<sup>11,14</sup> which was associated with cardiac dysfunction progressing with age.<sup>14</sup> Those observations, and pre-clinical findings of LV hypertrophy<sup>15</sup> and myocardial

fibrosis,<sup>9</sup> reflect the compromised metabolic flexibility in inborn errors of long-chain fatty acid  $\beta$ -oxidation.<sup>16</sup> In a clinical trial, subclinical reductions in myocardial mass and improvements in LV function upon supplementation with triheptanoin were reported for LCFAOD patients in absence of baseline cardiac complications.<sup>17</sup> Combined, those reports suggest that morphological and functional changes of the LCFAOD heart can develop under normal, well-fed conditions.

Case reports of cardiac manifestations in LCFAOD patients predominantly describe rapid-onset symptoms during metabolic crises.<sup>18,19</sup> In current practice, echocardiography and electrocardiography (ECG) are used for cardiac follow-up of LCFAOD patients. The frequency of and clinical indication for these investigations are based on expert opinion, which is not evidence-based.<sup>20</sup> As such, it is unclear if subclinical morphological and/or functional abnormalities of the heart exist in LCFAOD patients. This knowledge may be essential to guide treatment for preventing severe complications. In this work, we used state-of-the-art MRI and <sup>1</sup>H-MRS to obtain quantitative measures of heart morphology and contractile function, fibrosis, and myocardial lipid content in adult LCFAOD patients. Results were compared with matched control subjects to determine if there are any abnormalities in the LCFAOD heart.

## 2 | METHODS

### 2.1 | Study population

We performed an observational case-control study in adult LCFAOD patients and gender-, age-, and BMI-matched control subjects. Patients ( $n = 14$ ; 2 LCHADD, 4 CPT2D, and 8 VLCADD) were recruited via their treating metabolic physician between December 2015 and August 2018, with data on the clinical history available for all patients. All patients were diagnosed before inclusion of LCFAODs in the Dutch newborn screening program in 2007, of whom 11 were diagnosed after presenting with clinical symptoms and 3 after establishing diagnosis in a sibling. A comprehensive description of the Dutch VLCADD patient population has recently been published,<sup>3</sup> and an up-to-date national overview of diagnosed LCFAOD cases is available at [www.ddrmd.nl](http://www.ddrmd.nl). Matched control subjects ( $n = 14$ ) were recruited via flyers. All participants underwent the MR protocol as described below. The study was approved by the local institutional review board (NL41971.018.12; Academic Medical Center, University of Amsterdam, Amsterdam, The Netherlands) and participants provided written informed consent in accordance with the Declaration of Helsinki.

### 2.2 | Enzyme activity and long-chain fatty acid $\beta$ -oxidation flux

All patients included in the present study were fully characterized at the enzyme and molecular level. This included the quantitative assessment of VLCAD, CPT2, and LCHAD activity in lymphocytes as described previously,<sup>21</sup> determination of the rate of oleate  $\beta$ -oxidation in intact skin fibroblasts<sup>22</sup> and Sanger sequencing of the ACADVL, CPT2, and HADHA genes.

### 2.3 | MR protocol

Subjects were examined using a comprehensive noninvasive cardiac MR protocol that included functional cine MRI, <sup>1</sup>H-MRS, MR tagging, and native  $T_1$  and  $T_2$  relaxometry. All examinations were conducted on an Ingenia 3 Tesla MR system (Philips, Best, The Netherlands). A detailed description of the MR protocol and data analyses is provided in Supporting Information.

First, cine MRI of the heart was performed to obtain two- and four-chamber long-axis views of the LV. A stack of 12 to 15 contiguous short-axis slices covering the LV was acquired for the quantification of LV and right ventricular (RV) volumes and myocardial mass.

Next, <sup>1</sup>H-MRS of the interventricular septum (Figure 4) was performed as described previously,<sup>23</sup> using a single-voxel point-resolved spectroscopy (PRESS) sequence. Water-suppressed spectra ( $8 \times 8$  acquisitions) were acquired at an echo time (TE) of 40 ms and a long repetition time (TR) of  $>6$  seconds to minimize partial saturation effects for signal quantification, interleaved with acquisitions of 8 unsuppressed water spectra at a TR of  $>9$  seconds (water at 4.7 ppm on-resonance) for metabolite quantification reference.

Then, MR tagging was performed to allow for a detailed assessment of LV myocardial contractile function. An orthogonal grid (grid spacing, 7 mm) was applied prior to the acquisition of five parallel short-axis slices.

Subsequently,  $T_2$  and  $T_1$  relaxometry was used for myocardial tissue characterization with a multi-echo gradient spin-echo sequence (8 echoes; TE,  $18 + 7 \times 9$  ms) and a modified Look-Locker inversion recovery (MOLLI) sequence, respectively.

### 2.4 | MR data analyses

#### 2.4.1 | Cine MRI

We quantified LV and RV cavity volumes and myocardial mass via segmentation of the LV and RV walls in the cine

MR images by manually delineating the ventricular endocardial and epicardial contours using QMass 8.1 (Medis medical imaging systems BV, Leiden, The Netherlands).<sup>24</sup> Measured parameters included the LV and RV end-diastolic volumes (EDV), end-systolic volumes (ESV), stroke volumes (SV), ejection fractions (EF), global longitudinal strain (GLS), mid-cavity LV wall thickness, and LV and RV myocardial masses. Volume and mass parameters were indexed to body surface area (BSA).<sup>25</sup>

### 2.4.2 | <sup>1</sup>H-MRS

Spectral fitting was performed in the time-domain using AMARES in jMRUI.<sup>26</sup> Myocardial lipid content was quantified as the percentage of the sum of the triglyceride signal amplitudes over the unsuppressed water signal amplitude. Creatine content in the myocardium was estimated by expressing the creatine-methyl signal amplitude as a percentage of the unsuppressed water signal amplitude.

### 2.4.3 | MR tagging

Myocardial contractile mechanics were assessed by an analysis of tagged short-axis MR images as described previously,<sup>27</sup> yielding quantifications of LV torsion and endocardial circumferential strain. Torsion during contraction follows from the larger radius for epicardial cardiomyocytes compared to endocardial cardiomyocytes, and the myofiber architecture of opposing helical orientations going from the subendocardial to the subepicardial LV wall.<sup>28</sup> In the normal heart, a fixed degree of torsion per amount of ejection is required to achieve a homogeneous distribution of cardiomyocyte contraction across the myocardial wall. This notion can be captured by calculating the ratio of LV torsion and circumferential strain (ie, shortening) during the ejection phase. This torsion-to-shortening ratio (TSR) was found to be consistent across experiments in dogs<sup>29</sup> and humans.<sup>27</sup> Torsion and shortening time curves were used to derive peak torsion, peak shortening, and the TSR during myocardial contraction.

### 2.4.4 | Tissue T<sub>2</sub> and T<sub>1</sub> relaxometry

Quantification of myocardial T<sub>2</sub> and T<sub>1</sub> relaxation time constants was done with QMap 2.2 (Medis medical imaging systems BV) for a region of interest drawn in the interventricular septum.

## 2.5 | Statistical analyses

Results of individual patients were compared with their matched controls. Data for patient and control groups are presented as median (range). Differences between patients and matched controls were tested with the Wilcoxon signed-rank test, with the level of significance set at  $P < .05$ . Analyses were performed using SPSS 24.0 (SPSS, Inc., Chicago, Illinois).

## 3 | RESULTS

### 3.1 | Subject characteristics

Clinical data for the patients are summarized in Table 1. VLCADD#1 and VLCADD#3 as well as VLCADD#6 and VLCADD#8 were siblings. VLCADD#2 was matched with her sister as a control subject. Evaluation of the cardiac history revealed that one patient (VLCADD#1) had reversible HCM at the time VLCADD was diagnosed at infancy and an episode of cardiac decompensation with low EF at age 15 years. One patient (VLCADD#5) had hypertension and mild subvalvular aortic stenosis.

### 3.2 | LV and RV morphology and function

We quantified LV and RV morphology and function with volumetric analyses of cine MRI series, and made paired comparisons of the patient cohort with the group of matched control subjects (Table 2). In LCFAOD patients, LV myocardial mass/BSA was higher than in controls ( $P = .011$ ; Figure 1). Three patients had abnormally high LV myocardial mass/BSA values<sup>30</sup>: CPT2D#4 (78.4 g/m<sup>2</sup>), LCHADD#2 (85.4 g/m<sup>2</sup>), and VLCADD#1 (101.7 g/m<sup>2</sup>). RV myocardial mass/BSA was not different between patients and control subjects, nor were any of the other RV parameters. LV EDV, ESV, and SV were similar for patients and controls. The LV mass-to-volume ratio was higher for LCFAOD patients ( $P = .008$ ; Figure 1), which was most pronounced in the CPT2D patients. LV EF was similar for patients and control subjects (64 [41-76] vs 64 [54-76] %,  $P = 0.397$ ; Table 2), although LV EF was low for VLCADD#1 (41%). This was mirrored by similar GLS for patients and control subjects (−21.8 [−31.6 to −15.0] vs −20.8 [−25.3 to −15.0] %,  $P = .463$ ; Table 2), with the most depressed GLS found in VLCADD#1 (−15.0%). Combined, these data indicate some hypertrophic LV remodeling without a systematic global impairment of LV systolic performance in LCFAOD patients.

**TABLE 1** Individual characteristics for long-chain fatty acid β-oxidation deficient patients

Patient	Gender	Age (y)	Age at diagnosis (y)	BMI (kg/m <sup>2</sup> )	Dietary fat (En%)	Mutations	Flux	Enzyme activity (7%) <sup>a</sup>	Cardiac history
LCHADD#1	F	28	0	23.4	17 En% (71% LCT/29% MCT)	c.1528G>C(p.Glu510Gln) c.1678C>T (p.Arg560*)	32%		None
LCHADD#2	M	19	0	19.5	30 En% (61% LCT/39% MCT)	c.1528G>C(p.Glu510Gln) c.1712 T>C(p.Leu571Pro)	32%	20%	None
CPT2D#1	M	47	11	28.4	24 En%, MCT used during illness	c.338C>T (p.Ser113Leu) c.1891C>T (p.Arg631Cys)	NA	10%	None
CPT2D#2	M	49	17	24.5	NR	c.338C>T (p.Ser113Leu) c.338C>T (p.Ser113Leu)	NA	28%	None
CPT2D#3	M	54	47	29.5	NR, MCT used during illness	c.338C>T (p.Ser113Leu) c.338C>T (p.Ser113Leu)	NA	22%	None
CPT2D#4	M	57	41	26.6	31 En% (76% LCT/24% MCT)	c.338C>T (p.Ser113Leu) c.370C>T (p.Arg124Val)	NA	17%	Hypertension
VLCADD#1 <sup>b</sup>	F	21	0	20.6	38 En% (21% LCT/79% MCT)	c.104delC (p.Pro35LeufsX26) c.104delC (p.Pro35LeufsX26)	7%	<5%	0 y: transient HCM 15 y: transient HCM with transition to DCM
VLCADD#2	F	22	0	34.8	NR	c.848 T>C(p.Val283Ala) c.1141_1143delGAG (p.Glu381del)	32%	5%	None
VLCADD#3 <sup>b</sup>	M	18	0	21.1	20 En% (30% LCT/70% MCT)	c.104delC (p.Pro35LeufsX26) c.104delC (p.Pro35LeufsX26)	6%	<5%	None
VLCADD#4	M	23	19	22.7	NR, MCT used during illness	c.541dupC (p.His181ProfsX72) c.1072A>G (p.Lys358Glu)	51%	6%	None
VLCADD#5	M	38	28	26.7	Fat restriction, no MCT	c.877C>T (p.His293Tyr) c.1322G>A (p.Gly441Asp)	33%	5%	Hypertension, mild subvalvular aortic stenosis
VLCADD#6 <sup>c</sup>	M	42	35	26.3	NR	c.848 T>C (p.Val283Ala) c.1444_1448delAAGGA (p.Lys482AlafsX78) and c.1509_1514delAAGAGG (p.Glu504_Ala505del)	69%	9%	None
VLCADD#7	M	44	26	26.9	32 En% (63% LCT/37% MCT)	c.520G>A (p.Val174Met) c.833_835delAAG (p.Lys278del)	33%	12%	Hypertension

(Continues)

TABLE 1 (Continued)

Patient	Gender	Age (y)	Age at diagnosis (y)	BMI (kg/m <sup>2</sup> )	Dietary fat (En%)	Mutations	Flux	Enzyme activity	Cardiac history
VLCADD#8 <sup>c</sup>	M	46	39	23.7	NR	c.848 T>C (p.Val283Ala) c.1444_1448delAAGGA (p.Lys482AlafsX78) and c.1509_1514delAGAGG (p.Glu504_Ala505del)	44%	12%	None

Note: Enzyme activity (lymphocytes) and long-chain fatty acid  $\beta$ -oxidation flux (skin fibroblasts) are indicated as a percentage of healthy control values.

Abbreviations: CPT2D, carnitine palmitoyltransferase II deficiency; En%, energy intake derived from fat, as a percentage of total energy intake; F, female; LCHADD, long-chain 3-hydroxyacyl-CoA dehydrogenase deficiency; LCT, long-chain triglyceride; M, male; MCT, medium-chain triglyceride; NA, not available; NR, no dietary restrictions; VLCADD, very long-chain acyl-CoA dehydrogenase deficiency.

<sup>a</sup>Measured in skin fibroblasts.

<sup>b</sup>Siblings.

<sup>c</sup>Siblings.

### 3.3 | High LV torsion in LCFAOD patients

Figure 2 illustrates that absolute LV torsion was typically higher in the LCFAOD patients compared to control subjects ( $-0.18$  [ $-0.25$  to  $-0.11$ ] vs  $-0.14$  [ $-0.21$  to  $-0.11$ ] rad,  $P = .026$ ). In only two (LCHADD#2 and VLCADD#1) out of 14 patients was LV torsion lower than in their control subjects. Particularly, VLCADD#1, who has a history of cardiomyopathy (Table 1), had the lowest LV torsion of all subjects. Consistent with the normal LV EF we observed in all but one patient (VLCADD#1), circumferential shortening was similar in patients and controls ( $P = .875$ ; Figure 2). Combined with a higher LV torsion, this translated into a higher TSR in patients compared to control subjects ( $P = .006$ ), suggesting a transmural imbalance in cardiomyocyte contractility in LCFAOD patients.

### 3.4 | Myocardial T<sub>1</sub> and T<sub>2</sub> relaxometry

Native myocardial T<sub>1</sub> values were similar in LCFAOD patients and controls (1174 [1145-1310] vs 1190 [1059-1232] ms,  $P = .875$ ; Figure 3). Concomitant to our findings for LV myocardial mass and LV torsion, patients LCHADD#2 and VLCADD#1 were most deviant, with the highest myocardial T<sub>1</sub> values of all subjects (1306 ms and 1310 ms, respectively), which may point to myocardial fibrosis in these patients. Myocardial T<sub>2</sub> values were similar for patients and control subjects (41 [36-54] vs 43 [37-49] ms,  $P = .944$ ).

### 3.5 | Myocardial metabolite levels

We used localized <sup>1</sup>H-MRS to quantify myocardial lipid levels and total creatine content relative to the total water signal. Metabolite content could not be quantified for two patients (CPT2D#2 and VLCADD#5) due to low spectral quality. We did not find a difference in myocardial lipid content between LCFAOD patients and matched controls (0.73 [0.20-2.22] vs 0.71 [0.25-2.39] %,  $P = 1.0$ ; Figure 4). Myocardial total creatine content was similar for patients and control subjects (0.12 (0.06-0.15) vs 0.11 (0.11-0.14) %,  $P = .308$ ; Table 2).

## 4 | DISCUSSION

Cardiomyopathy can be a life-threatening complication in patients with LCFAOD. Until now, little is known about the effects of LCFAOD on the adult human heart,

**TABLE 2** Characteristics and MR results for long-chain fatty acid  $\beta$ -oxidation deficient patients and matched control subjects

	LCFAOD patients (n = 14)	Matched control subjects (n = 14)	P-value
Female (n)	3	3	
Age (y)	41 (18-57)	38 (18-60)	.706
BMI (kg/m <sup>2</sup> )	25 (20-35)	25 (19-34)	.975
BSA (m <sup>2</sup> )	2.00 (1.66-2.21)	2.04 (1.64-2.51)	.198
LV mass/BSA (g/m <sup>2</sup> )	68.1 (48.9-101.7)	57.0 (42.9-73.5)	<b>.011</b>
LV EDV/BSA (mL/m <sup>2</sup> )	69.4 (57.1-111.2)	65.9 (54.1-79.9)	.363
LV ESV/BSA (mL/m <sup>2</sup> )	29.6 (21.0-66.4)	27.8 (22.6-40.3)	.331
LV SV/BSA (mL/m <sup>2</sup> )	39.7 (28.7-54.5)	37.0 (27.3-51.0)	.510
LV EF (%)	64 (41-76)	64 (54-76)	.397
LV mass-to-volume ratio (g/mL)	0.94 (0.79-1.14)	0.83 (0.70-1.05)	<b>.008</b>
LV wall thickness (mm)	9.3 (7.5-11.6)	8.2 (7.0-9.9)	<b>.004</b>
LV GLS (%)	-21.8 (-31.6 to -15.0)	-20.8 (-25.3 to -15.0)	.463
Torsion (rad)	-0.18 (-0.25 to -0.11)	-0.14 (-0.21 to -0.11)	<b>.026</b>
Circumferential shortening (-)	-0.30 (-0.46 to -0.16)	-0.31 (-0.35 to -0.24)	.875
TSR (rad)	0.50 (0.53-0.80)	0.42 (0.27-0.67)	<b>.006</b>
RV mass/BSA (g/m <sup>2</sup> )	22.9 (16.7-27.8)	20.7 (16.4-27.8)	.268
RV EDV/BSA (mL/m <sup>2</sup> )	60.1 (48.8-88.6)	66.2 (44.7-93.0)	.761
RV ESV/BSA (mL/m <sup>2</sup> )	22.8 (15.0-46.3)	30.6 (16.5-45.6)	.268
RV SV/BSA (mL/m <sup>2</sup> )	37.8 (26.1-52.7)	35.2 (26.7-51.7)	.670
RV EF (%)	61 (45-74)	55 (50-70)	.091
LV mass/RV mass (-)	3.2 (2.1-3.7)	2.8 (1.9-3.7)	<b>.049</b>
T <sub>2</sub> (ms)	41 (36-54)	43 (37-49)	.944
Native T <sub>1</sub> (ms)	1175 (1145-1310)	1190 (1059-1232)	.875
Myocardial lipid content (% of water signal)	0.73 (0.20-2.22)	0.71 (0.25-2.39)	1.000
Myocardial creatine content (% of water signal)	0.12 (0.06-0.15)	0.11 (0.11-0.14)	.308

Note: Values indicate median (range), with P-values reported for Wilcoxon signed-rank tests.

The level of significance was set at  $P < .05$ , represented in bold values.

Abbreviations: BMI, body mass index; BSA, body surface area; EDV, end-diastolic volume; EF, ejection fraction; ESV, end-systolic volume; GLS, global longitudinal strain; LV, left ventricle; RV, right ventricle; TSR, torsion-to-shortening ratio.

and regular follow-up of the heart is generally not implemented.<sup>31</sup> Our detailed quantitative assessment of the myocardium and its contractile performance with MR methods revealed subclinical differences in the hearts of 14 adult LCFAOD patients compared to the hearts of matched control subjects. LV myocardial mass was higher, albeit moderately, in most patients compared to their controls, with three patients showing LV hypertrophy. Moreover, LV torsion during ejection was higher in patients than in control subjects, whereas circumferential shortening was similar. Myocardial T<sub>1</sub> was high in two patients with LV hypertrophy, which may be indicative of diffuse myocardial fibrosis. Furthermore, our measurements of myocardial lipid levels with <sup>1</sup>H-MRS did not reveal evidence of in vivo myocardial lipid accumulation.

LCFAOD patients can present with severe HCM or DCM during metabolic derangements, which may reverse upon treatment.<sup>32</sup> Here, we found a higher LV myocardial mass and a higher LV myocardial mass-to-volume ratio compared to their matched controls for essentially all patients. Because we focused on adult patients in this study, our cohort may be skewed toward cases with a relatively mild phenotype, particularly for the CPT2D patients. Our data show that, even in mild and/or stable LCFAOD patients, hypertrophic remodeling of the myocardium can occur while systolic function in terms of LV EF and GLS remains normal.

The normal circumferential shortening in combination with the higher LV torsion that we observed in LCFAOD patients is indicative of a transmural imbalance of myofiber contractility, which may be caused by a

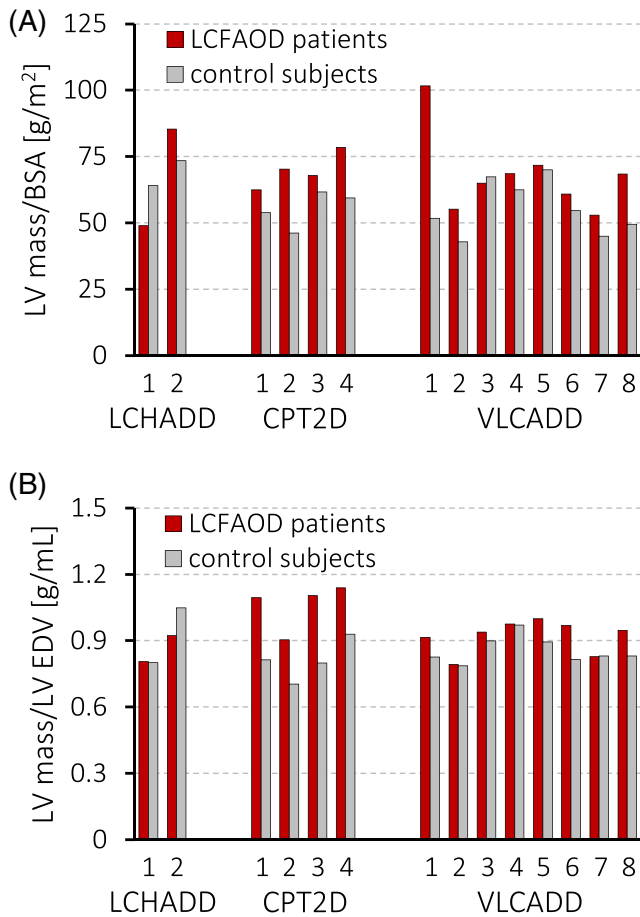


**FIGURE 1** LV morphology. Left ventricular (LV) myocardial mass/BSA. A, and LV mass-to-volume ratios. B, measured with cine MRI in long-chain fatty acid  $\beta$ -oxidation deficient (LCFAOD) patients ( $n = 14$ ) and gender-, age-, and BMI-matched control subjects ( $n = 14$ ). Individual values are presented. BSA, body surface area; CPT2D, carnitine palmitoyltransferase II deficiency; LCHADD, long-chain 3-hydroxyacyl-CoA dehydrogenase deficiency; VLCADD, very long-chain acyl-CoA dehydrogenase deficiency

compromised energy homeostasis. It is known that the subendocardium is more vulnerable to subtle pathologic processes such as impairments of myocardial perfusion and the development of fibrosis.<sup>33</sup> As a consequence, the transmural contractile homogeneity of a healthy heart is lost, increasing LV torsion. Such loss of myofiber contractile function in the subendocardium relative to the subepicardium is reflected by an increase in TSR. Previously, Hollingsworth et al<sup>34</sup> found a moderate correlation of TSR increasing with age. We carefully matched our control subjects with the patients, precluding any age-, gender-, or BMI-related causes of the differences we observed. Myocardial  $T_1$ , as a measure of diffuse tissue fibrosis, was similar to the matched controls for all patients in which high peak torsion was found, suggesting that fibrosis is not the cause of any contractile

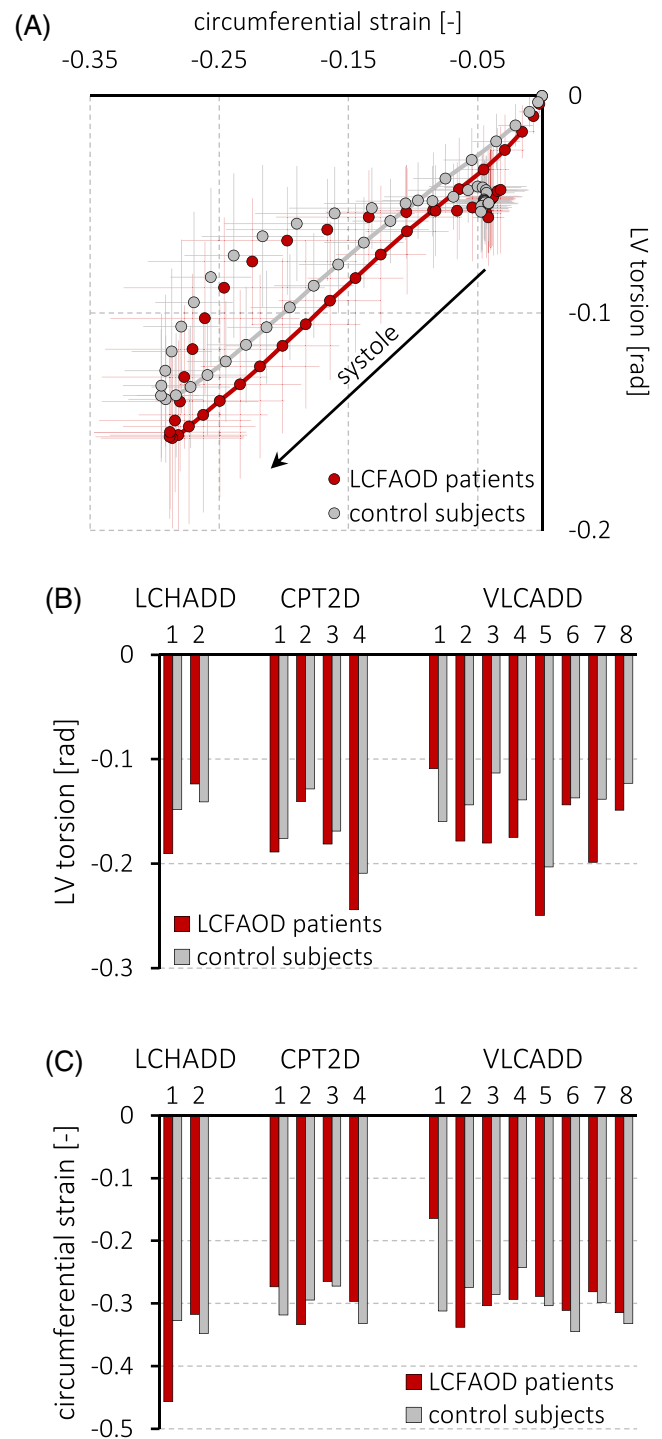


**FIGURE 2** MR tagging. Left ventricular (LV) circumferential strain (ie, shortening) plotted against LV torsion throughout the cardiac cycle. A, The direction of time is indicated with the arrow, showing a linear trajectory during systole reflecting the torsion-to-shortening ratio (TSR). Absolute torsion was higher ( $P = .026$ ) in long-chain fatty acid  $\beta$ -oxidation deficient (LCFAOD) patients than in matched controls, B, whereas LV circumferential shortening was similar ( $P = .875$ ). C, Negative LV torsion indicates a counterclockwise rotation of the apex relative to the base, when viewed from the apex.<sup>27</sup> CPT2D, carnitine palmitoyltransferase II deficiency; LCHADD, long-chain 3-hydroxyacyl-CoA dehydrogenase deficiency; VLCADD, very long-chain acyl-CoA dehydrogenase deficiency



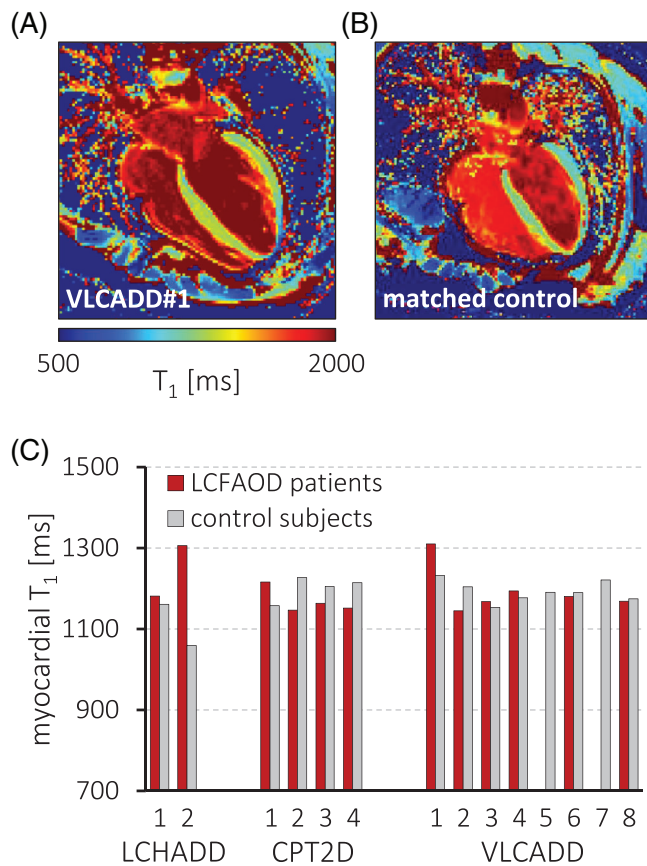


**FIGURE 3** Myocardial  $T_1$ . Native  $T_1$  maps of patient VLCADD#1, A, and her matched control, B, Myocardial  $T_1$  was 1310 ms vs 1235 ms for VLCADD#1 and control, respectively. Myocardial  $T_1$  for most other patients was similar to control values ( $P = .875$ ). C, except for LCHADD#2 (1306 ms). CPT2D, carnitine palmitoyltransferase II deficiency; LCHADD, long-chain 3-hydroxyacyl-CoA dehydrogenase deficiency; VLCADD, very long-chain acyl-CoA dehydrogenase deficiency

dysfunction. Instead, we propose that an inadequate metabolic flexibility and a chronically compromised myocardial energy homeostasis<sup>14,16</sup> may therefore be the governing factors for the transmural difference in myocardial contractile function in LCFAOD, rather than fibrosis or reduced myocardial perfusion that occurs in normal aging or type 2 diabetes.<sup>27,35</sup> Whereas phosphorus-31 MRS ( $^{31}\text{P}$ -MRS) has been used to identify a disturbed energy homeostasis in skeletal muscle of VLCADD patients,<sup>36</sup> the current state of cardiac  $^{31}\text{P}$ -MRS may not yet be sensitive enough to confirm a myocardial energy deficiency in a relatively small cohort of LCFAOD patients with direct measurements of in vivo myocardial phosphocreatine and ATP levels.<sup>37</sup>

Notably, in two LCFAOD patients, LV hypertrophy was accompanied by high native  $T_1$  values. Native  $T_1$  correlates well with the collagen volume fraction,<sup>38</sup> and is a surrogate marker for diffuse myocardial fibrosis.

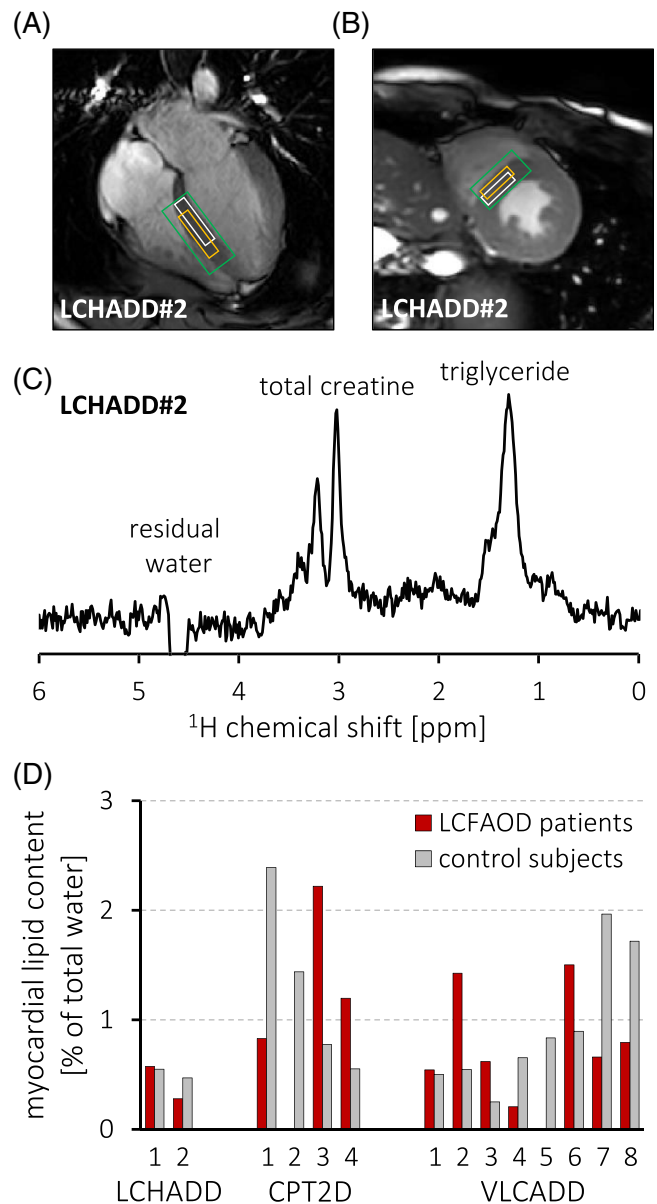


**FIGURE 4** Localized proton magnetic resonance spectroscopy ( $^1\text{H}$ -MRS) of the myocardium. A voxel (other box) with the chemical shift-displaced voxel for creatine (white box) was positioned in the septum, A,B, enclosed by the shim volume (green box). Using water-suppressed single-voxel point-resolved spectroscopy (PRESS), a  $^1\text{H}$ -MR spectrum, C, was acquired to estimate myocardial lipid content, D, and total creatine content. CPT2D, carnitine palmitoyltransferase II deficiency; LCHADD, long-chain 3-hydroxyacyl-CoA dehydrogenase deficiency; VLCADD, very long-chain acyl-CoA dehydrogenase deficiency

Although we did not administer a gadolinium-based contrast agent in this study, a quantitative evaluation of the extracellular volume fraction via contrast-enhanced  $T_1$  mapping may be considered for specific cases such as the patients with high native myocardial  $T_1$  values we identified here. Moreover, in both of these patients LV torsion

was low compared to their controls, which was opposite to the findings in the other patients. The combination of a high myocardial  $T_1$  and low LV torsion could point to a fibrotic tissue structure in these patients<sup>39</sup> and may indicate a more progressed state of disease. Indeed, one of these patients (VLCADD#1) had developed LV systolic functional impairments evidenced by a low EF (41%), depressed GLS (-15.0%), and low circumferential shortening (-0.16).

We found no evidence for overt *in vivo* myocardial lipid accumulation in the present study. These findings are in apparent contrast to reported findings in a LCFAOD mouse model<sup>12</sup> and in pediatric autopsies.<sup>7,8</sup> Here, we found a rather broad range of myocardial lipid levels in patients and control subjects. Caloric restriction is known to influence myocardial lipid content.<sup>40</sup> We did not restrict nutritional intake in this study, because a prolonged fasting period is undesirable for LCFAOD patients. All patients remained on their individual diet that varied from normal fat intake to restricted long-chain triglyceride (LCT) intake and/or medium-chain triglyceride (MCT) supplementation (Table 1).<sup>20,41</sup> In LCFAOD mouse models, myocardial lipid accumulation accompanied by cardiac dysfunction was found under stressed conditions.<sup>12,14</sup> Tucci et al showed that long-term MCT supplementation in a VLCADD mouse model led to a severely disturbed whole-body lipid homeostasis and a near doubling of myocardial triglyceride concentrations associated with decreased EF and DCM.<sup>14,42</sup> Importantly, in well fed conditions, EF still progressively declined in the absence of myocardial lipid accumulation, suggesting that lipotoxicity is not the main contributor to the development of cardiac disease in those LCFAOD mice.<sup>14</sup> Our observations in adult LCFAOD patients are consistent with those animal studies.

The clinical relevance of the observed subtle abnormalities in these adult LCFAOD hearts is unknown and remains to be established in longitudinal studies. Particularly, the noninvasive and quantitative nature of our MR methods would allow for such comprehensive follow-up investigations. Apart from symptom monitoring, low-frequency (eg, once every 5 years) MRI examinations to evaluate heart function and myocardial fibrosis formation can be considered for adult VLCADD and LCHADD patients. Echocardiography may suffice in CPT2D patients, because native  $T_1$  values were not abnormal for CPT2D patients in the current cohort. Moreover, no cardiac complications in adult CPT2D patients have been reported to date. This screening interval can be shortened in case of complaints and/or signs that are compatible with reduced heart function. There should be increased awareness of signs of cardiac decompensation or arrhythmia at times of metabolic

crises, also in patients with previously normal heart morphology and function.

## 5 | CONCLUSIONS

In conclusion, we identified subclinical morphological and functional differences between the hearts of LCFAOD patients and their gender-, age-, and BMI-matched controls using state-of-the-art MR methods. Our results suggest a chronic cardiac disease phenotype and adaptive hypertrophic remodeling of the heart in LCFAOD, potentially triggered by a mild, but chronic, energy deficiency. MR data may provide sensitive quantitative outcome measures for longitudinal investigations of LCFAOD, even in asymptomatic patients with a subclinical phenotype.

## ACKNOWLEDGMENTS

We thank all subjects for participating in this study. We thank Dr. Paul de Heer for his contribution to the implementation of the <sup>1</sup>H-MRS data acquisition and processing protocol. Parts of this work were presented at the fifth Annual International Network for Fatty Acid Oxidation Research and Management (INFORM) Symposium (Honorable Mention), and at the Society for the Study of Inborn Errors of Metabolism (SSIEM) Annual Symposium, Athens, Greece, in September 2018. Dr. Bakermans is supported a Veni grant from the Netherlands Organisation for Scientific Research (NWO; project number 91617155). The authors confirm independence from the sponsor, and the content of the article has not been influenced by the sponsor.

## CONFLICT OF INTEREST

All authors declare that they have no conflict of interest.

## AUTHOR CONTRIBUTIONS

Gepke Visser, S. Matthijs Boekholdt, and Adrianus J. Bakermans designed research. Suzan J. G. Knottnerus, Jeannette C. Bleeker, Mirjam Langeveld, Gepke Visser, Frits A. Wijburg, S. Matthijs Boekholdt, and Adrianus J. Bakermans recruited study participants. Suzan J. G. Knottnerus, Jeannette C. Bleeker, Aart J. Nederveen, and Adrianus J. Bakermans acquired MR data, and Sacha Ferdinandusse provided biochemical data. Gustav J. Strijkers, S. Matthijs Boekholdt, and Adrianus J. Bakermans analyzed MR data. Suzan J. G. Knottnerus, and Adrianus J. Bakermans performed statistical analyses. Suzan J. G. Knottnerus, Gepke Visser, and Adrianus J. Bakermans drafted the manuscript. Dr. Adrianus J. Bakermans serves as guarantor for the article, accepts full responsibility for the work and the

conduct of the study, had access to the data, and controlled the decision to publish. All authors reviewed and approved the final manuscript.

## DATA AVAILABILITY STATEMENT

The datasets generated and analyzed during the current study are available from the corresponding author on reasonable request.

## ORCID

Adrianus J. Bakermans  <https://orcid.org/0000-0001-9291-9441>

## REFERENCES

- Houten SM, Violante S, Ventura FV, Wanders RJA. The biochemistry and physiology of mitochondrial fatty acid beta-oxidation and its genetic disorders. *Annu Rev Physiol*. 2016;78:23-44.
- Knottnerus SJG, Bleeker JC, Wüst RCI, et al. Disorders of mitochondrial long-chain fatty acid oxidation and the carnitine shuttle. *Rev Endocr Metab Disord*. 2018;19:93-106.
- Bleeker JC, Kok IL, Ferdinandusse S, et al. Impact of newborn screening for very long-chain acyl-CoA dehydrogenase deficiency on genetic, enzymatic and clinical outcomes. *J Inherit Metab Dis*. 2019;42:414-423.
- Baruteau J, Sachs P, Broue P, et al. Clinical and biological features at diagnosis in mitochondrial fatty acid beta-oxidation defects: a French pediatric study of 187 patients. *J Inherit Metab Dis*. 2013;36:795-803.
- Nakamura M, Sadoshima J. Cardiomyopathy in obesity, insulin resistance and diabetes. *J Physiol*. 2019. <https://doi.org/10.1113/JP276747>.
- North KN, Hoppel CL, De Girolami U, Kozakewich HP, Korson MS. Lethal neonatal deficiency of carnitine palmitoyltransferase II associated with dysgenesis of the brain and kidneys. *J Pediatr*. 1995;127:414-420.
- Aliefendioğlu D, Dursun A, Coşkun T, Akçören Z, Wanders RJA, Waterham HR. A newborn with VLCAD deficiency. Clinical, biochemical, and histopathological findings. *Eur J Pediatr*. 2007;166:1077-1080.
- Bleeker JC, Visser G, Wijburg FA, Ferdinandusse S, Waterham HR, Nikkels PGJ. Severe fat accumulation in multiple organs in pediatric autopsies: an uncommon but significant finding. *Pediatr Dev Pathol*. 2017;20:269-276.
- Kurtz DM, Rinaldo P, Rhead WJ, et al. Targeted disruption of mouse long-chain acyl-CoA dehydrogenase gene reveals crucial roles for fatty acid oxidation. *Proc Natl Acad Sci U S A*. 1998;95:15592-15597.
- Exil VJ, Roberts RL, Sims H, et al. Very long-chain acyl-coenzyme a dehydrogenase deficiency in mice. *Circ Res*. 2003;93:448-455.
- Xiong D, He H, James J, et al. Cardiac-specific VLCAD deficiency induces dilated cardiomyopathy and cold intolerance. *Am J Physiol Heart Circ Physiol*. 2014;306:H326-H338.
- Bakermans AJ, Geraedts TR, van Weeghel M, et al. Fasting-induced myocardial lipid accumulation in long-chain acyl-CoA dehydrogenase knockout mice is accompanied by impaired left ventricular function. *Circ Cardiovasc Imaging*. 2011;4:558-565.
- Bakermans AJ, van Weeghel M, Denis S, Nicolay K, Prompers JJ, Houten SM. Carnitine supplementation attenuates myocardial lipid accumulation in long-chain acyl-CoA dehydrogenase knockout mice. *J Inherit Metab Dis*. 2013;36:973-981.
- Tucci S, Flögel U, Hermann S, Stürm M, Schafers M, Spiekerkoetter U. Development and pathomechanisms of cardiomyopathy in very long-chain acyl-CoA dehydrogenase deficient (VLCAD<sup>-/-</sup>) mice. *Biochim Biophys Acta*. 2014;1842:677-685.
- Cox KB, Liu J, Tian L, Barnes S, Yang Q, Wood PA. Cardiac hypertrophy in mice with long-chain acyl-CoA dehydrogenase or very long-chain acyl-CoA dehydrogenase deficiency. *Lab Invest*. 2009;89:1348-1354.
- Bakermans AJ, Dodd MS, Nicolay K, Prompers JJ, Tyler DJ, Houten SM. Myocardial energy shortage and unmet anaplerotic needs in the fasted long-chain acyl-CoA dehydrogenase knockout mouse. *Cardiovasc Res*. 2013;100:441-449.
- Gillingham MB, Heitner SM, Martin J, et al. Triheptanoin versus trioctanoin for long-chain fatty acid oxidation disorders: a double blinded, randomized controlled trial. *J Inherit Metab Dis*. 2017;40:831-843.
- Katz S, Landau Y, Pode-Shakked B, et al. Cardiac failure in very long-chain acyl-CoA dehydrogenase deficiency requiring extracorporeal membrane oxygenation (ECMO) treatment: a case report and review of the literature. *Mol Genet Metab Rep*. 2017;10:5-7.
- Kluge S, Kühnelt P, Block A, et al. A young woman with persistent hypoglycemia, rhabdomyolysis, and coma: recognizing fatty acid oxidation defects in adults. *Crit Care Med*. 2003;31:1273-1276.
- Spiekerkoetter U, Lindner M, Santer R, et al. Treatment recommendations in long-chain fatty acid oxidation defects: consensus from a workshop. *J Inherit Metab Dis*. 2009;32:498-505.
- Wanders RJ, Ruiten JP, IJlst L, Waterham HR, Houten SM. The enzymology of mitochondrial fatty acid beta-oxidation and its application to follow-up analysis of positive neonatal screening results. *J Inherit Metab Dis*. 2010;33:479-494.
- Olpin SE, Manning NJ, Pollitt RJ, Clarke S. Improved detection of long-chain fatty acid oxidation defects in intact cells using [9,10-<sup>3</sup>H]oleic acid. *J Inherit Metab Dis*. 1997;20:415-419.
- de Heer P, Bizino MB, Lamb HJ, Webb AG. Parameter optimization for reproducible cardiac <sup>1</sup>H-MR spectroscopy at 3 tesla. *J Magn Reson Imaging*. 2016;44:1151-1158.
- Schulz-Menger J, Bluemke DA, Bremerich J. al. Standardized image interpretation and post processing in cardiovascular magnetic resonance. *J Cardiovasc Magn Reson*. 2013;15:35.
- Du Bois D, Du Bois EF. A formula to estimate the approximate surface area if height and weight be known. *Arch Intern Med (Chic)*. 1916;XVII:863-871.
- Vanhamme L, van den Boogaart A, Van Huffel S. Improved method for accurate and efficient quantification of MRS data with use of prior knowledge. *J Magn Reson*. 1997;129:35-43.
- Lumens J, Delhaas T, Arts T, Cowan BR, Young AA. Impaired subendocardial contractile myofiber function in asymptomatic aged humans, as detected using MRI. *Am J Physiol Heart Circ Physiol*. 2006;291:H1573-H1579.

28. Omar AM, Vallabhajosyula S, Sengupta PP. Left ventricular twist and torsion. *Circ Cardiovasc Imaging*. 2015;8:e003029.
29. Arts T, Veenstra PC, Reneman RS. Epicardial deformation and left ventricular wall mechanisms during ejection in the dog. *Am J Physiol*. 1982;243:H379-H390.
30. Petersen SE, Aung N, Sanghvi MM, et al. Reference ranges for cardiac structure and function using cardiovascular magnetic resonance (CMR) in Caucasians from the UKbiobank population cohort. *J Cardiovasc Magn Reson*. 2017;19:18.
31. Laforêt P, Acquaviva-Bourdain C, Rigal O, et al. Diagnostic assessment and long-term follow-up of 13 patients with very long-chain acyl-coenzyme a dehydrogenase (VLCAD) deficiency. *Neuromuscul Disord*. 2009;19:324-329.
32. Saudubray JM, Martin D, de Lonlay P, et al. Recognition and management of fatty acid oxidation defects: a series of 107 patients. *J Inherit Metab Dis*. 1999;22:488-502.
33. Stanton T, Marwick TH. Assessment of subendocardial structure and function. *JACC Cardiovasc Imaging*. 2010;3:867-875.
34. Hollingsworth KG, Blamire AM, Keavney BD, Macgowan GA. Left ventricular torsion, energetics, and diastolic function in normal human aging. *Am J Physiol Heart Circ Physiol*. 2012;302:H885-H892.
35. Enomoto M, Ishizu T, Seo Y, et al. Subendocardial systolic dysfunction in asymptomatic normotensive diabetic patients. *Circ J*. 2015;79:1749-1755.
36. Diekman EF, Visser G, Schmitz JP, et al. Altered energetics of exercise explain risk of rhabdomyolysis in very long-chain acyl-CoA dehydrogenase deficiency. *PLoS One*. 2016;11:e0147818.
37. Bakermans AJ, Bazil JN, Nederveen AJ, et al. Human cardiac <sup>31</sup>P-MR spectroscopy at 3 tesla cannot detect failing myocardial energy homeostasis during exercise. *Front Physiol*. 2017;8:939.
38. Nakamori S, Dohi K, Ishida M, et al. Native T<sub>1</sub> mapping and extracellular volume mapping for the assessment of diffuse myocardial fibrosis in dilated cardiomyopathy. *JACC Cardiovasc Imaging*. 2018;11:48-59.
39. Taylor RJ, Umar F, Lin ELS, et al. Mechanical effects of left ventricular midwall fibrosis in non-ischemic cardiomyopathy. *J Cardiovasc Magn Reson*. 2016;18:1.
40. van der Meer RW, Hammer S, Smit JW, et al. Short-term caloric restriction induces accumulation of myocardial triglycerides and decreases left ventricular diastolic function in healthy subjects. *Diabetes*. 2007;56:2849-2853.
41. Bleeker JC, Kok IL, Ferdinandusse S, et al. Proposal for an individualized dietary strategy in patients with very long-chain acyl-CoA dehydrogenase deficiency. *J Inherit Metab Dis*. 2018;42:159-168.
42. Tucci S, Flögel U, Sturm M, Borsch E, Spiekerkoetter U. Disrupted fat distribution and composition due to medium-chain triglycerides in mice with a beta-oxidation defect. *Am J Clin Nutr*. 2011;94:439-449.

### SUPPORTING INFORMATION

Additional supporting information may be found online in the Supporting Information section at the end of this article.

**How to cite this article:** Knottnerus SJG, Bleeker JC, Ferdinandusse S, et al. Subclinical effects of long-chain fatty acid  $\beta$ -oxidation deficiency on the adult heart: A case-control magnetic resonance study. *J Inherit Metab Dis*. 2020;43:969–980. <https://doi.org/10.1002/jimd.12266>